Equivalent Roughness Height for Plane Bed under Steady Flow

Benoît Camenen, Ph.D.[1]; Atilla Bayram, A.M.ASCE[2]; and Magnus Larson[3]

Abstract: This paper presents a new relationship between the roughness height and the main hydrodynamic and sediment parameters for plane beds under steady current conditions. In order to derive such a formula, a large data base involving plane-bed experiments was compiled from previous investigations and analyzed. Comparisons between the data and different existing predictive formulas for the bed roughness obtained from the literature were also made. A relationship with the Shields parameter only, which is commonly proposed, appeared to be insufficient. The roughness was also found to be a function of a Froude number and a dimensionless settling velocity. A critical Shields parameter was identified up to which the equivalent roughness ratio is proportional to the Shields parameter. The new empirical equation that was developed yields the best results for all conditions investigated, and should improve the understanding of the total shear stress.

DOI: 10.1061/(ASCE)0733-9429(2006)132:11(1146)

CE Database subject headings: Roughness; Shear stress; Sheet flow; Experimental data; Steady flow.

Introduction

Estimating the sediment transport rate in rivers is highly important in connection with irrigation, water supply, and flood protection. However, sediment transport rate predictions suffer from insufficient understanding of resistance to flow in alluvial channels. Although the roughness height remains quite difficult to estimate, it is a fundamental parameter for determining sediment transport. Numerical models to calculate the sediment transport rate in the river or coastal environment often employ relationships which depend on the Shields parameter, especially to estimate the bed load transport. The bed roughness is an important input parameter in the Shields number, and it is usually unknown even for steady current conditions.

In general, owing to dimensional reasons, the bed roughness height of a flat and fixed bed is given in terms of the Nikuradse roughness height. It is supposed to be on the order of the median grain diameter or of some larger grain size percentiles ($k_s = 1-5$ times d_{50}, d_{65}, d_{84}, or d_{90} according to the literature). However, the value of k_s varies considerably depending on the configuration of the grains forming the roughness of the flow boundaries. At high Shields parameter, bed forms disappear and the sediment moves along the bottom mainly in a layer denoted as sheet flow. The presence of a relatively thin sheet-flow layer with high sediment concentration markedly affects the flow above it. One important aspect of the presence of a sheet layer is the increased roughness, compared to a situation without such a layer (Wilson 1966; Sumer et al. 1996). Under sheet-flow conditions, the roughness height may be several orders of magnitude larger than for a fixed bed. This is probably caused by the increased energy dissipation in the sheet-flow layer, because of interaction between individual sediment grains as well as between the sediment and the fluid. It is often assumed that the roughness height under sheet- flow conditions is on the order of the sheet flow layer thickness (Wilson 1987; Van Rijn 1993). Wilson (1966) performed a series of tests in a pressurized conduit in order to obtain high shear stress values. Based on these results, he proposed a relationship between the roughness and the Shields parameter [see Eq. (2) in Table 1]. Some more recent studies (Nnadi and Wilson 1992; Sumer et al. 1996) confirm this relationship with the Shields parameter. However, only a few experiments were performed in a "realistic" environment, i.e., an open channel. Thus, one question is how significant are the effects of the setup in these specific experiments. Moreover, for coarser sediment, even if the sheet flow layer was not observed, the bed load sediment transport appeared to significantly affect the velocity profile and thus the roughness (Smart 1999). Given the extensive laboratory and field data set that was compiled in this study, a more comprehensive analysis was possible.

The main objective of the present study is to propose a new relationship for the equivalent roughness height to better estimate the prediction of the total shear stress. Many data sets were employed in the development of the formula, covering a wide range of hydrodynamic and sediment transport conditions. Also, comparisons were made with several existing formulas from the literature to quantify the improvement in the predictions offered by the new formula. The first part of the paper summarizes previous studies and introduces the data sets utilized in the present work, whereas the second part discusses the influence of the main governing parameters on the roughness heights and how these were combined to yield the new formula.

[1]Dept. of Water Resources Engineering, Lund Univ., Box 118, S-221 00 Lund, Sweden (corresponding author). E-mail: bencamenen@yahoo.com

[2]Senior Coastal Engineer, Han-Padron Associates, 22 Cortlandt St., New York, NY 10007.

[3]Dept. of Water Resources Engineering, Lund Univ., Box 118, S-221 00 Lund, Sweden.

Note. Discussion open until April 1, 2007. Separate discussions must be submitted for individual papers. To extend the closing date by one month, a written request must be filed with the ASCE Managing Editor. The manuscript for this paper was submitted for review and possible publication on July 25, 2003; approved on January 30, 2006. This paper is part of the ***Journal of Hydraulic Engineering***, Vol. 132, No. 11, November 1, 2006. ©ASCE, ISSN 0733-9429/2006/11-1146–1158/$25.00.

Table 1. Relationships for Equivalent Roughness for Steady Current Sheet Flow as They Chronologically Appeared in Literature

Author(s)	Relationship	Eq.
Wilson (1987)	$\frac{k_s}{d_{50}}=5\theta$	(2)
Yalin (1992)	$\frac{k_s}{d_{50}}=5\theta+(\theta-4)^2(0.043\theta^3-0.289\theta^2-0.203\theta+0.125)$	(3)
Van Rijn (1993)	$\frac{k_s}{d_{90}}=3\theta$	(4)
Sumer et al. (1996)	$\frac{k_s}{d_{50}}=\begin{cases}2+0.6\theta^{2.5} & \text{if } \varpi>0.9 \\ 4.5+\frac{1}{8}\exp(0.6W_*^4)\theta^{2.5} & \text{if } \varpi\leq 0.9\end{cases}$	(5*a*) (5*b*)
Bayram et al. (2003)	$\frac{k_s}{d_{50}}=\max(2.5,2.5\theta^{1.5})$	(6)

Existing Equivalent Roughness Height Relationships

In general, the main problem of bed roughness prediction under sheet flow conditions is that the roughness height depends on the flow variables and the sediment transport rate. In the literature, several existing relationships for equivalent roughness under sheet flow conditions have been investigated (see Table 1). Most of the existing formulas assume a relationship between an equivalent roughness ratio (ratio between the roughness height k_s and a characteristic grain size d) and the Shields parameter based on the total shear stress θ

$$\frac{k_s}{d} \propto \theta \tag{1}$$

In Table 1 d_{50} and d_{90}=median diameter and the diameter for which 90% of sediment (by weight) is smaller, respectively; W_*=nondimensional settling velocity defined by Sumer et al. (1996); and ϖ_s=suspension parameter. Shields parameter, nondimensional settling velocity, and suspension parameter are defined by, respectively

$$\theta = \frac{u_*^2}{(s-1)gd_{50}} \tag{2}$$

$$W_* = \frac{W_s}{\sqrt{(s-1)gd_{50}}} \tag{3}$$

$$\varpi_s = \frac{W_s}{u_*} \tag{4}$$

in which u_*=bed friction velocity; s=relative density of sediment grains ($s=\rho_s/\rho_w$ where ρ_s and ρ_w=density of sediment grains and fluid, respectively); g=acceleration due to gravity; and W_s=settling velocity.

Wilson (1966, 1987, 1989) studied the roughness height in the sheet flow regime using high concentrations of slurry and experiments performed in pressurized closed conduits. He used two different types of material: sand particles with a median diameter of d_{50}=0.7 mm, and nylon particles with a median diameter of d_{50}=3.9 mm. Based on the experimental results, Wilson proposed a simple relationship [Eq. (2) in Table 1] where the roughness height is proportional to the Shields parameter and the median sediment diameter. Yalin (1992) re-examined Wilson's (1987) data and proposed a new relationship to fit this data set, which yielded Eq. (3) (in Table 1).

Van Rijn (1993) used data from Einstein and Chien (1955) and Winterwerp et al. (1990) to compute roughness height under sheet- flow conditions including the effect of the sediment particles on the viscosity in the near bed region where the concentration is high. Van Rijn (1993) assumed that the viscosity of the mixture in the near bed region is ten times higher than that of clear water and proposed Eq. (4) (in Table 1) which involves the Shields parameter and d_{90}.

Sumer et al. (1996) carried out extensive flume experiments in order to investigate velocity and concentration profiles inside and outside the sheet-flow layer of movable beds, using four kinds of sediment. They confirmed that flow resistance due to the sheet-flow layer could be expressed in terms of the ratio between Nikuradse's equivalent roughness height and d_{50}, and the Shields parameter. Eq. (5*a*) and (5*b*) (in Table 1) was derived through empirical fitting toward their data involving a power dependence of k_s/d_{50} on θ. Sumer et al. (1996) showed that, in the case of suspension mode ($\varpi_s<0.8-1.0$), the roughness height depends not only on the Shields parameter θ, but also on the parameter W_*.

A clear indication from all the above formulas is that the ratio of roughness height to particle diameter increases with increasing Shields parameter values. This is mainly because of an increase in the k_s value for high-concentration flows due to enhanced interaction between sediment particles in the near bed region. Thus, the particle velocities are greatly reduced by the collisions within the bed and between each other resulting in relatively large differences between the local fluid and particle velocity. The associated fluid drag forces are the driving forces for the particle motion. Conversely, these drag forces are reducing the fluid velocity, which can be interpreted as a shear effect in addition to the fluid shear.

Steady Plane-Bed Data Set

Background

To investigate roughness height under plane-bed conditions, a wide range of existing data sets were compiled and analyzed. Table 2 summarizes these data sets, where the type of flow motion and sediment properties are listed. The seventh and eighth

Table 2. Data Summary for Plane-Bed Conditions

Author(s)	Flow type	Number	Material	s	d_{50} (mm)	W_*	ϖ_s	F
Gilbert (1914)	Steady uniform flow, flume, plane bed	250[a]	Sand	2.65	0.3	0.65	0.78–1.08	0.95–1.30
			Sand	2.65	0.4	0.73	0.81–1.30	0.92–1.83
			Sand	2.65	0.5	0.82	0.87–1.58	0.79–2.08
			Sand	2.65	0.8	0.91	1.06–1.92	1.09–2.08
			Sand	2.65	3.2	1.01	2.68–3.90	0.99–1.49
			Sand	2.65	4.9	1.02	2.92–4.08	0.81–1.38
U.S. Waterways Experiment Station (1935, –1936)	Steady uniform flow, flume, plane bed	162[a]	Sand	2.65	0.18–4.1	0.41–1.01	1.47–5.84	0.42–0.76
Wilson (1966)	Pressured closed conduit	101	Nylon	1.14	3.9	0.99	0.55–0.90	0.80–1.00
			Sand	2.65	0.7	0.90	0.35–0.87	2.24–3.35
Kamphuis (1974)	Steady uniform flow, flume, fixed plane bed	12	Sand	2.65	0.5–46	0.73–1.03	1.5–22	0.29–1.19
Yalin (1977)	Steady uniform flow, flume, fixed plane bed	53	Sand	2.65	6.3	1.02	5.3–20.8	0.30–0.54
Brownlie (1981)	Various experimental data, plane bed	339[a]	Plastic	1.30–1.41	2.2–20.2	0.97–1.02	1.23–6.47	0.02–0.57
			Sand	2.49–2.67	0.088–20	0.16–1.02	0.12–10.5	0.08–3.51
Brownlie (1981)	Various field data, plane bed	40[a]	Sand	2.65	0.084–7.0	0.15–1.02	0.13–5.39	0.13–0.53
Smart (1984, 1999) with Nikora (1999)	Exp. for steep channels and field data, plane bed	140[a]	Sand	2.65	2.0–10.5	1.02	0.55–3.44	1.09–2.93
			Gravel	2.65	53–200	1.00–1.02	0.65–19.8	0.41–1.01
Rickenmann (1991)	Flume, hyperconcentrated sand–water–clay mixture	58	Gravel	1.95–2.65	10.0	1.02	0.81–2.12	1.53–2.84
Nnadi and Wilson (1992)	Pressured closed conduit	105[a]	Bakelite	1.57	0.67	0.59	0.26–0.43	1.96–3.41
			Bakelite	1.54	1.05	0.79	0.30–0.58	1.73–4.14
			Sand	2.67	0.70	0.80	0.29–0.90	1.73–2.98
			Nylon	1.14	3.94	0.99	0.57–0.91	0.70–1.10
Van Rijn (1993)	Flume, rigid plane bed	17	Sand	2.65	0.12–0.94	0.25–0.94	0.08–0.99	0.89–1.99
Coleman and Melville (1996)	Field data, plane bed	34	Sand	2.65	0.21	0.45	0.68–1.33	0.31–0.63
			Sand	2.65	0.82	0.97	1.65–3.96	0.38–0.88
Sumer et al. (1996)	Flume, hyperconcentrated sand–water mixture	158	Plastic	1.27	3.00	1.33	0.82–1.69	0.82–1.27
			Plastic	1.14	2.60	1.32	0.57–1.31	0.76–1.01
			Acrylic	1.13	0.60	0.72	0.30–1.17	0.26–0.68
			Sand	2.65	0.13	0.26	0.17–0.29	0.75–1.20
Julien and Raslan (1998)	Laboratory flume	28	Sand	2.50	0.20	0.44	0.44–0.69	0.67–0.96
			Sand	2.70	0.60	0.85	1.95–2.44	0.49–0.91
			Sand	2.60	0.40	0.73	0.93–1.46	0.69–1.03

[a]Sediment transport data also available.

columns in the table show the nondimensional settling velocity W_* [cf. Eq. (3)], defined by Sumer et al. (1996), and the suspension parameter ϖ_s [cf. Eq. (4)], respectively. In the ninth column, the Froude number is presented defined as

$$\mathsf{F} = \frac{U_c}{\sqrt{gh}} \tag{5}$$

where U_c=mean velocity of the steady current and h=water depth. The Soulsby equation (1997) was used to estimate the settling velocity W_s of the particles when it was not measured.

A total number of around 1,500 experimental cases from more than 14 different sources were analyzed to determine Nikuradse's equivalent sand roughness k_s. Many of these cases were obtained from the compilation of alluvial channel data presented by Brownlie (1981). Only data corresponding to a plane-bed regime were included in the present analysis, involving experiments from both the laboratory and the field. The laboratory data originated from Gilbert (1914), U.S. Waterways Experiment Station (1935, 1936), Singh (1960), Guy et al. (1966), Neill (1967), Williams (1970), and Willis et al. (1972), whereas the field data came from Colby and Hembree (1955; the Niobrara River) and Culbertson et al. (1972; the Rio Grande conveyance). The kinematic viscosity was assumed to be equal to 1.0×10^{-6} m^2/s when it was not provided by the writers. When the water temperature was known, ν was estimated using the equation proposed by Ahrens (2000).

These data sets can be classified into four main types according to the experimental procedure used:

- Field data;
- Laboratory flume data;
- Pressured closed conduit data; and
- Hyperconcentrated sand–fluid mixture data.

The extensive data set summarized in Table 2 displays the following general characteristics:

- The Froude number is typically lower for field than for laboratory conditions;
- Field observations of the Froude number for plane bed range between 0.3 and 1.3;
- Comparatively, higher values of the Froude number were em-

ployed in the laboratory, typically, 1.0–3.6; and

- The suspension parameter, ϖ_s, shows a wide range of values between 0.1 and 5.4 both for the field and the laboratory data.

The wide range of values for these hydraulic and sediment parameters should allow for a better understanding of the physics governing the roughness height over a plane bed.

Different Plane-Bed Regimes

Two main plane-bed regimes can be distinguished:

1. The lower plane-bed regime where the bed can be regarded as fixed. The roughness height has been found to correspond to the coarser fraction of the bed sediment size distribution (Sleath 1984, Van Rijn 1993). This plane regime occurs generally for low shear stress ($\theta < 0.05-0.1$) before the appearance of ripples.
2. The upper plane-bed regime where strong sediment transport occurs and a layer of sediment generally moves collectively (sheet flow). This regime occurs when ripples and dunes disappear and the roughness height is strongly affected by the sediment transport. Observations made during sheet flow experiments showed that the effective grain roughness of a sheet flow bed is on the order of the sheet flow layer thickness or the boundary layer thickness (Wilson 1987). The upper plane bed is limited to the appearance of antidunes if the Froude number exceeds unity.

For practical purposes, it may be assumed that the upper plane-bed regime starts when the Shields parameter is greater than 0.8 (i.e., $\theta > 0.8$). However, this relationship was proposed for fine sediment (which was used in the sheet flow experiments) and corresponds to the disappearance of the bed forms. Van Rijn (1984) identified the upper regime using a dimensionless particle diameter and a transport stage parameter that expresses the ratio between excess grain shear stress and the critical shear stress for initiation of motion. He found the limit for the upper plane-bed regime to be

$$T = \frac{\theta - \theta_{cr}}{\theta_{cr}} = 25 \tag{6}$$

where θ_{cr}=critical Shields parameter for initiation of motion. Following this equation, the upper plane-bed regime is reached when $\theta = 0.8-3$ depending on the grain size. In case of gravel bed rivers, Smart (1999) showed that the mobile bed significantly affects the velocity profiles. However, this type of bed cannot be compared with the sheet-flow bed observed with finer sediment. Nevertheless, it should correspond to the upper plane-bed regime as the roughness is no longer only a function of the grain size.

Sumer et al. (1996) showed that two sheet-flow regimes exist in accordance with the mode of sediment transport that is with or without suspension (see Fig. 1). Based on their data they also found that the value at which suspension mode starts to occur, namely θ being between 0.6 and 2.0 depending on the sediment size, correlates well with a certain value on the ratio between settling velocity and shear velocity $\varpi_s \approx 0.8-1.0$. Therefore, for larger Shields numbers (i.e., $\varpi_s < 0.8-1.0$), the grains are transported not only in the sheet flow layer but also in suspension. However, the critical value of ϖ_s is subject to some uncertainty related to the sediment used (density, grain shape, and grain size distribution). Roughness characteristics during the no-suspension mode were examined by selecting a critical value of $\varpi_s = 0.9$ for the present data set. When $\varpi_s < 0.8-1.0$, Sumer et al. (1996) proposed an empirical relationship for the roughness height that is an increasing function of the parameter W_*.

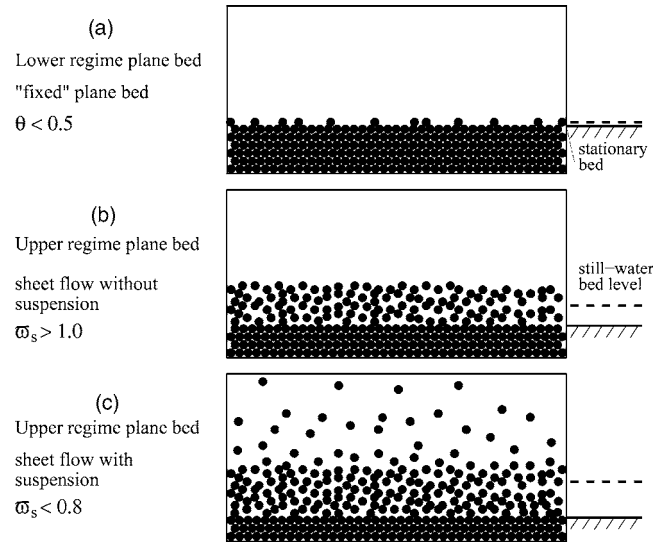

Fig. 1. Schematic pictures illustrating three main plane-bed regimes (after Sumer et al. 1996)

Computation of Roughness Height

Nikuradse's Equivalent Sand Roughness

The main method to compute the roughness height is through the shear velocity obtained from flow resistance measurements. By assuming that other mechanisms for energy dissipation besides the bottom friction were negligible in the experiments, the measurements from the different sources were employed to derive bed friction velocity and then the corresponding roughness height was calculated. In steady flow, the resistance can be expressed in terms of the Nikuradse's equivalent sand roughness, k_s, which for rough turbulent flows may be calculated using Nikuradse's resistance relationship (Yalin 1977; Schlichting 1979), as soon as $k_s \ll R_b$

$$\frac{U_c}{u_*} = \frac{1}{\kappa} \ln\left(\frac{A_b R_b}{k_s}\right) \tag{7}$$

in which U_c [$=Q/(bh)$]=mean velocity; $\kappa \approx 0.41$=von Karman constant; $A_b \approx 11$=constant assuming a fully turbulent flow; and R_b=hydraulic radius associated with the bed. Here, Q=flow discharge; b=flume width; and h=flow depth. Also, in the above equation u_* denotes the bed friction velocity obtained from

$$u_* = \sqrt{g R_b I_e} \tag{8}$$

in which I_e=energy slope. Note that R_b is calculated using the method of Vanoni and Brooks (Van Rijn 1993), where wall correction (for the sidewalls) is made.

Eqs. (7) and (8) yield a roughness height of

$$k_s = \frac{A_b R_b}{\exp\left(\kappa \frac{U_c}{\sqrt{g R_b I_e}}\right)} \tag{9}$$

Thus, k_s=function of the three measured variables h (R_b=function of h and the geometry of the channel), U_c and I_e.

Grain Shear Reynolds Number

Eq. (7) assumes a hydraulically rough flow, that is, a grain shear Reynolds number $\mathsf{R}_* > 70$, where

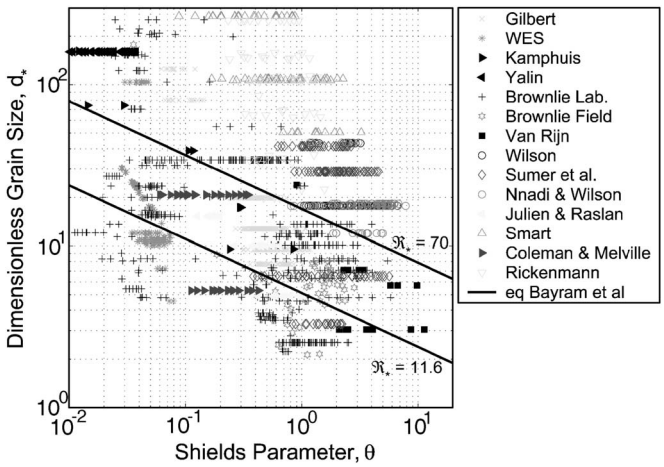

Fig. 2. Dimensionless grain size d_* versus Shields parameter θ

$$\mathsf{R}_* = \frac{u_* d_{50}}{\nu} \tag{10}$$

Julien and Raslan (1998) investigated the influence of this parameter on the resistance to flow for the upper plane-bed regime. They proposed empirical formulas according to two types of boundary conditions based on R_*. Fig. 2 presents the dimensionless grain size d_* versus the Shields parameter θ for the whole data set, where

$$d_* = \sqrt[3]{\frac{(s-1)g}{\nu^2}} d_{50} \tag{11}$$

In Fig. 2, solid lines are used to separate the data points belonging to different flow regimes including transition to hydraulically smooth boundary for $\mathsf{R}_*=11.6$ and transition to hydraulically rough boundary for $\mathsf{R}_*=70$. It is noted that some of the data points clustered under hydraulically smooth boundary conditions. Inside the hydraulically smooth boundary the effect of the laminar sublayer thickness is dominant and viscosity is no longer negligible. Thus, the value A_b in Eq. (7) is not a constant anymore but a function of R_*. Therefore, an overestimation of the calculated roughness is induced through Eq. (7) since the value used for A_b is too large. However, these critical values of R_* to differentiate smooth flow from rough flow were established for a fixed bed and supposing $k_s=d_{50}$. In most of the cases presented in this paper, a movable bed is present, which modifies the flow significantly. Also, in computing the grain shear Reynolds number using k_s instead of d_{50} (which is more accurate) only 10% of the data remain under the smooth flow limit and 60% of the data correspond to rough flow ($\mathsf{R}_{*b}=u_* k_s/\nu > 70$).

Sumer et al. (1996) computed the roughness height for their experimental data from both flow resistance [Eq. (7)] and velocity profile measurements. Although some of their data involved a flow hydraulically smooth [R_* computed according to Eq. (10), i.e., using d_{50}], they found that both methods are in fairly good agreement, except for small values of the roughness height ($k_s/d_{50}<4$). Furthermore, the error induced in the computation of the constant A_b in Eq. (7) is less than 50% depending of R_* [A_b varies from approximately 15 to 40 for a smooth or transitional flow; see Yalin (1977)]. Uncertainties in determining the hydraulic radius R_b (and thus the shear velocity u_*) may cause larger errors than assuming A_b constant in Eq. (7) for the calculation of k_s. In addition, it should be remembered that most of the time, the logarithmic velocity distribution might only be a "good approximation" and uncertainties associated with this assumption will induce scatter in the results mainly for small values of roughness height.

However, in order to avoid the influence of viscosity on the results, only data cases where the flow is hydraulically rough were kept in the following study (smooth boundary cases where $\mathsf{R}_*<11.6$ were neglected).

Relative Submergence

Another hypothesis underlying Eq. (7) is that the relative submergence $k_s/h \ll 1$ [see Yalin (1977)]. However, in cases with large sediment diameters, often this hypothesis cannot be fulfilled. Indeed, in rivers with large bed material, the water depth h is only a few times larger than the sediment size (h value corresponds to a mean value). Most of the data from Smart and Rickenmann involve a relative submergence h/k_s close to 1 or even smaller than 1. Several authors (Whiting and Dietricht 1990; Ferro and Baiamonte 1994; Song et al. 1994; Smart 1999) found that a logarithmic profile can still be an accurate representation of the flow for these specific cases. The computation of the hydraulic roughness z_0 is nevertheless not obvious. Smart (1999) proposed defining the virtual bed level as the position where a time-averaged velocity profile would predict $u=0$. Then, z_0 describes the hydraulic roughness of the boundary ($u=0$ for $z=z_0$). The value of $k_s=30z_0$ does not have any physical basis but can still be used assuming that the logarithmic profile is approximately correct.

If the roughness elements are fully covered by the flow and a logarithmic profile extends to the surface, the depth-averaged velocity U_c is obtained by integrating the velocity profile over the flow depth (i.e., from $z=z_0$ to $z=z_0+R_b$)

$$\frac{U_c}{u_*} = \frac{1}{\kappa}\left[\left(\frac{R_b+z_0}{R_b}\right)\ln\left(\frac{R_b+z_0}{z_0}\right)-1\right] \tag{12}$$

As the length of wetted perimeter becomes imprecise where roughness elements are intricate or where they break the surface, Smart et al. (2002) proposed using the variable R_v instead of the hydraulic radius R_b. The radius R_v is defined as the volume of overlying water per unit plan area of bed. "For large relative roughness conditions the unit width or unit bed area used to evaluate R_v must contain a typical arrangement of roughness elements if it is to be representative. Where all roughness elements are covered by the flow, R_v becomes the average water depth h." Thus, to be coherent with Smart et al. (2002), R_b should be replaced in Eq. (12) by R_v-z_0. In situations where $k_s \ll h$, Eq. (12) simplifies to Eq. (7) with $A_b=11$.

In Fig. 3 is the roughness ratio found directly from the velocity profile plotted versus those obtained using Eq. (12) for the data from Nikora and Smart (1997). The two predictions are in fairly good agreement. Sumer et al. (1996) also showed that the estimation of the roughness height using the flow resistance measurements or the velocity profiles measurements are well correlated. This indicates the relevance of the flow resistance method to compute the roughness height.

Estimating Roughness Height

The roughness is calculated using Eq. (7) [Eq. (9)] if $k_s \leq 0.1h$ or Eq. (12) if $k_s > 0.1h$.

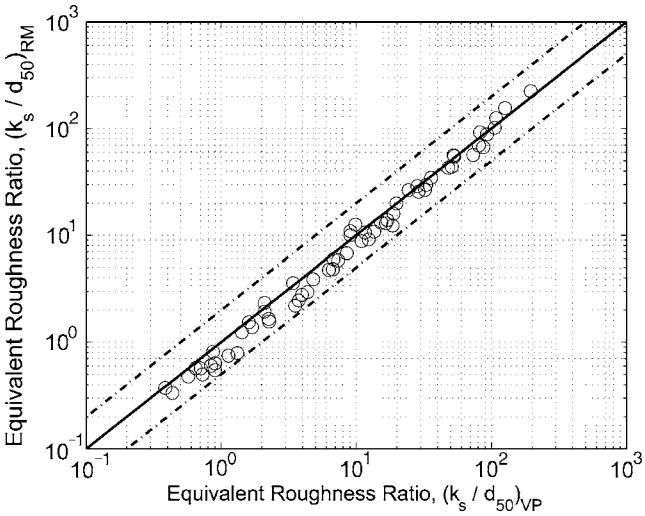

Fig. 3. Comparison of k_s/d_{50} found from velocity profile measurements (VP) with those obtained from flow resistance measurements (FR) using data from Nikora and Smart (1997)

Lower Plane-Bed Regime

In Fig. 4 is the ratio k_s/d_{90} plotted versus the ratio h/d_{90} following the study of Yalin (1977) for the data where the bed was fixed or where no or low sediment transport was observed (before bed forms occurred). These data encompass the studies of Kamphuis (1974), Yalin (1977), Neill (1967), Coleman and Melville (1996), and some of the data compiled by Brownlie (1981) including the data from the U.S. Waterways Experiment Station (1935, 1936) experiments. As previously observed by Kamphuis (1974) and Yalin (1977) the relative roughness ratio is scattered around a constant value of $k_s/d_{90}=2$ (or approximately $k_s/d_{50}=2.5$, smooth boundary cases excluded). The smooth boundary cases generally present a lower value of the relative roughness ratio ($k_s/d_{90}<1$) but viscosity is no longer negligible. These cases will be excluded for the following study.

Considering that the roughness height only corresponds to a geometric property, Yalin (1977) asserted that one should not infer that k_s is a function of the water depth. He also argued that

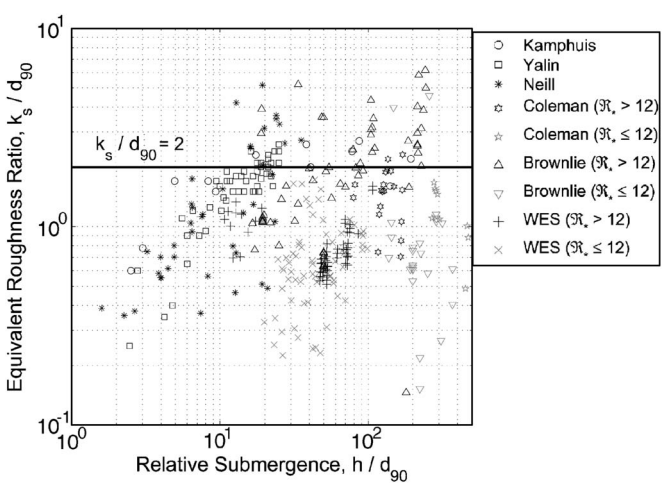

Fig. 4. Relation between roughness height k_s and grain size d_{90} versus ratio between water depth h and grain size d_{90} for lower regime plane bed

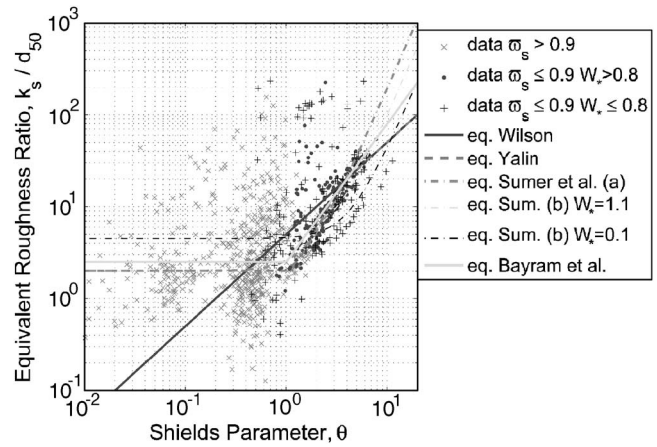

Fig. 5. Equivalent roughness ratio k_s/d_{50} versus total shear stress θ for data set together with predictions by formulas studied

the deviation clearly observed for $k_s/d_{90}<10$ is due to fact that the logarithmic velocity distribution is not applicable in this range. However, the study of Smart (1999) in a gravel bed river (where $k_s/d_{90}<10$) shows that a logarithmic profile is a good representation of the velocity profile and may even be extented over much of the water depth. The main reason for the scattering seems to be the "flow resistance method" utilized to compute the roughness that appears to be quite sensitive to the measurement accuracy.

From the selected data (smooth boundary cases excluded), assuming the roughness to be not only a geometrical parameter but also to depend on the flow, the roughness height appears to be an increasing function of the water depth when the relative depth $h/d_{90}<10$ (see Fig. 4). Spurious correlation may occur through Eq. (9) when calculating k_s and explain this relationship with the water depth. Nevertheless, assuming that the logarithmic profile correctly describes the velocity profile at the bottom, and since the variables h, U_c, and I_e are measured independently, it should not happen (see "Relative Submergence" and Fig. 3).

Upper Plane-Bed Regime—Comparison with Existing Formulas

In Fig. 5, the predicted values of the relative roughness ratio k_s/d_{50} for both field and laboratory data are plotted against the Shields number for all the cases in the hydraulically rough regime. This study includes cases where sediment transport is observed, which may influence the roughness height. The data points are separated in three groups: the first one corresponds to the no-suspension mode ($\varpi_s>0.9$), and the two others correspond to the suspension mode with $W_*>0.8$ or $W_*\leq 0.8$. In order to evaluate the performance of existing empirical relationships for the roughness height, predictions by the relationships studied are also plotted in the same graph. In the case of the Sumer et al. formula, three curves are plotted: Eq. (5*a*) (in Table 1) for the no-suspension mode (thick dashed-dotted line), and Eq. (5*b*) (in Table 1) for the suspension mode with $W_*=1.1$ and $W_*=0.1$ (fine gray and black dashed-dotted lines). In general, the figure shows that despite significant scatter, the roughness height increases with increasing Shields number. However, the roughness height can reach large values (ten to several hundred times the median grain size) even for relatively small values of the Shields parameter and in the no-suspension mode. The data in the figure also

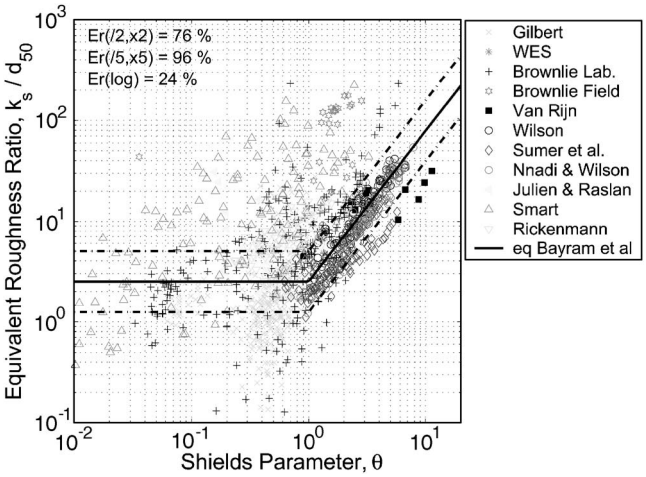

Fig. 6. Equivalent roughness ratio k_s/d_{50} versus total shear stress θ for different data sets studied together with Bayram et al. formula (dashed lines correspond to predictions within factor of two)

indicate the limits of the method used to compute the roughness height since several points yield a roughness height smaller than the median grain size of the sediment which is not realistic. Indeed, the method is quite sensitive to large values of the ratio U_c/u_* ($U_c/u_* > 15$).

The Yalin, Sumer et al., and Bayram et al. formulas give approximately the same results when the suspension mode is reached or the Shields parameter is larger than one (see Fig. 6) since these three formulas were calibrated with data from Wilson and Nnadi and Wilson, and also using the data from Sumer et al. for the two latter formulas. However the Sumer et al. formula tends to induce lower roughness height ratios when W_* is small. The data from Wilson and Nnadi and Wilson, and Sumer et al. are from experiments performed in physical models, which often imply large shear stresses and supercritical flows ($\mathsf{F} > 1$), whereas in nature, high shear stresses are usually associated with large depths and modest channel slopes (subcritical flows, $\mathsf{F} < 1$). This could explain the resulting scatter for the data from open channels as well as the dependence on the settling velocity as observed by Sumer et al. However, the Froude number has no significance for the tests with pressurized conduits, and the settling velocity, following the Sumer et al. study should only influence the results in the suspension mode. The slightly different results coming from the Wilson formula are explained by the fact that this relationship was only calibrated with high values of the Shields parameter (Bayram et al. 2003). In its present formulation, the Wilson formula is not suitable for $\theta < 0.3$ (see Fig. 5).

The larger scatter is observed for the no-suspension mode ($\varpi_s \leq 0.9$), which roughly corresponds to $\theta < 1-2$; and none of the formulas studied present good behavior. For these data, it seems that the Shields parameter is not the only parameter that affects the roughness height. Eq. (5*a*) (in Table 1) proposed by Sumer et al. (1996) appeared to have been fitted with data where $k_s/d_{50} < 10$ and is not confirmed by the results obtained using the other data set. It may also be noted than the Sumer et al. equation induces a discontinuity when $\varpi_s = 0.9$.

In Table 3, predictions of equivalent roughness within a factor of two and five of the measured values are presented for the different formulas and all data excluding data where $R_* \leq 12$ and where no sediment transport was observed. (Thus, "factor x" means between x times and $1/x$ times the measured roughness height.) There is poor agreement between all formulas and data within a factor of two (less than 60% of the data) and the formulas sometimes yield an error of up to two orders of magnitude. Accordingly, a logarithmic error index is proposed to establish a quantitative measure of agreement between formulas and data. The term "$\mathrm{Er}_{\log}$"(logarithmic error index) is defined as

Table 3. Prediction of Equivalent Roughness within Factor of Two and Five of Measured Values Together with Logarithmic Error Index for Formulas Studied and All Data

Author(s)	Predictions Factor 2 (%)	Predictions Factor 5 (%)	Logarithmic error (%)
Wilson	48	82	41
Yalin	62	86	34
Van Rijn	59	88	34
Sumer et al.	58	87	35
Bayram et al.	61	88	33
Eq. (15)	74	96	24

$$\mathrm{Er}_{\log} = \frac{100}{n}\sum_{1}^{n}\left|\log\left[\frac{(k_s/d_{50})_{\mathrm{num}}}{(k_s/d_{50})_{\mathrm{exp}}}\right]\right| \tag{13}$$

in which n denotes the number of observations.

The Wilson formula presents the poorest results mainly because it applies to the high-shear stress range, $\theta > 1$ (Wilson 1966). On the other hand, the Yalin, Sumer et al., and Bayram et al. formulas give very similar predictive results. However, all these formulas appear to be inadequate for some portions of the data set. In Fig. 6, the relative roughness ratio k_s is plotted versus the total shear stress θ, in order to distinguish different data sources used in analysis. The Bayram et al. formula is also plotted as a reference.

In Fig. 6, it can be observed that the Bayram et al. formula produces the largest errors for the data sets from Julien and Raslan, Smart, Brownlie (field data and some experimental data), and Rickenmann. The main characteristics of these data sets are that they were obtained for relatively small Shields numbers ($0.1 < \theta < 3$) with subcritical flows ($\mathsf{F} < 1$), whereas the Bayram et al. (2003) relationship is based on larger values of the Shields number ($1 < \theta < 10$) including mainly supercritical flows ($\mathsf{F} > 1$). Thus, as was observed by Wu and Wang (1999), the Froude number seems to be an important factor in roughness height predictions. Another important parameter which was introduced by Sumer et al. (1996) in case of the suspension mode is the settling velocity of the sediments.

Influence of Grain Size, Density, and Settling Velocity

Many authors showed that the roughness height is not only a function of the grain size and the Shields parameter. Sumer et al. (1996) found a relationship with the suspension parameter ϖ_s and the dimensionless settling velocity W_* [Eqs. (5*a*) and (5*b*) (in Table 1)]. Julien and Raslan (1998) observed an influence of the relative submergence h/d_{50} on the friction coefficient under steady currents. In this study, the influence of other parameters on the equivalent roughness ratio was observed such as the dimensionless grain size d_*, the relative sediment density s, the suspension parameter ϖ_s, the dimensionless settling velocities W_*, the relative submergence h/d_{50}, and the grain shear Reynolds number R_*. The correlation with the dimensionless grain size d_*, or more correctly with the settling velocity W_s (which is a function of d_*)

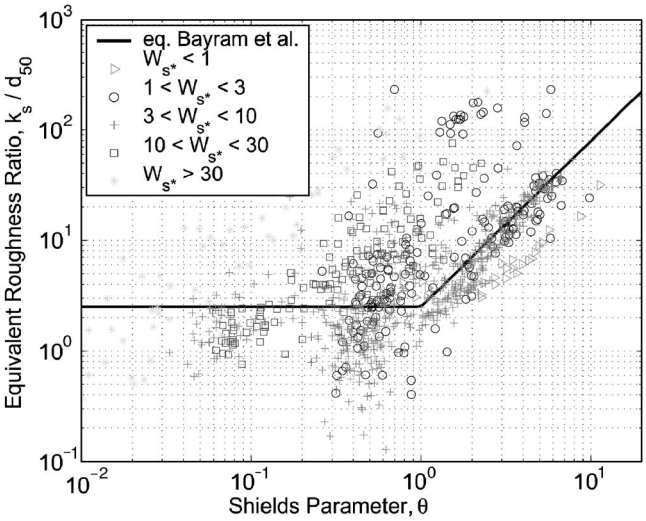

Fig. 7. Equivalent roughness ratio k_s/d_{50} versus total shear stress θ with respect to dimensionless settling velocity W_{s*} together with Bayram et al. formula

was the most significant. A correlation was thus observed with a new dimensionless settling velocity, introduced as follows:

$$W_{s*} = \left[\frac{(s-1)^2}{(g\nu)}\right]^{1/3} W_s \tag{14}$$

The influence of this parameter is clearly illustrated in Fig. 7. The higher W_{s*} is, the larger the equivalent roughness ratio is, even for a small Shields parameter. Sumer et al. relates the effect of the settling velocity on the roughness height ratio to the damping of turbulence induced by the suspended sediments, leading to a smaller flow resistance. For the no-suspension mode ($\varpi_s > 0.9$), the damping of turbulence may be due to the moving sediments (saltation) in the bed load layer. It should be noted that all the data where $0.05 < \theta < 0.8$ correspond to coarse sediment ($W_{s*} > 5$). In this range of values of the Shields parameter, the bed is expected to be covered with ripples but only when the sediment is sufficiently fine. For coarser sediment, ripples are seldom observed.

Table 4. Prediction of Equivalent Roughness within Factor of Two and Five of Measured Values Together with Logarithmic Error Index for Formulas Studied and All Data (Influence of Nondimensional Settling Velocity)

	$W_{s*} \leq 10$			$W_{s*} > 10$		
Author(s)	Pred. ×2 (%)	Pred. ×5 (%)	Er_{log} (%)	Pred. ×2 (%)	Pred. ×5 (%)	Er_{log} (%)
Wilson	57	89	32	16	60	73
Yalin	70	92	27	30	65	59
Van Rijn	64	90	31	41	81	44
Sumer et al.	65	92	30	32	67	57
Bayram et al.	68	92	30	33	67	56
Eq. (15)	70	95	26	86	99	17

Only larger bed forms may occur but were not observed by the authors of the specific data set compiled.

Table 4 presents the errors induced by the formulas studied with respect to different W_{s*} values. For $W_{s*} \leq 10$, results remain quite good for most of these formulas but when $W_{s*} > 10$, the predictions within a factor of two (5) agreement drops from approximately 65% (90%) to 35% (70%).

Influence of Froude Number

Another parameter which seems to influence the roughness height is the Froude number as observed in "Upper Plane-Bed Regime—Comparison with Existing Formulas." In order to clarify the effect of the Froude number on the roughness height, the relative roughness values k_s/d_{50} were plotted versus the total shear stress θ (cf. Fig. 8) with respect to four different ranges of the Froude number and using data sets where $W_{s*} \leq 10$ [cf. Fig. 8(a)] or $W_{s*} > 10$ [cf. Fig. 8(b)].

Fig. 8 shows that the relative roughness is a decreasing function of the Froude number, particularly for the data involving small Shields parameter values ($0.1 < \theta < 2$) or when $W_{s*} > 10$ [cf. Fig. 8(b)]. But it should be noted that the Froude number has no meaning for the experiments in pressured closed conduit data, as well as the data from Sumer et al. (1996) (the flume was covered with a lid at the top and acted as a pressurized "conduit"

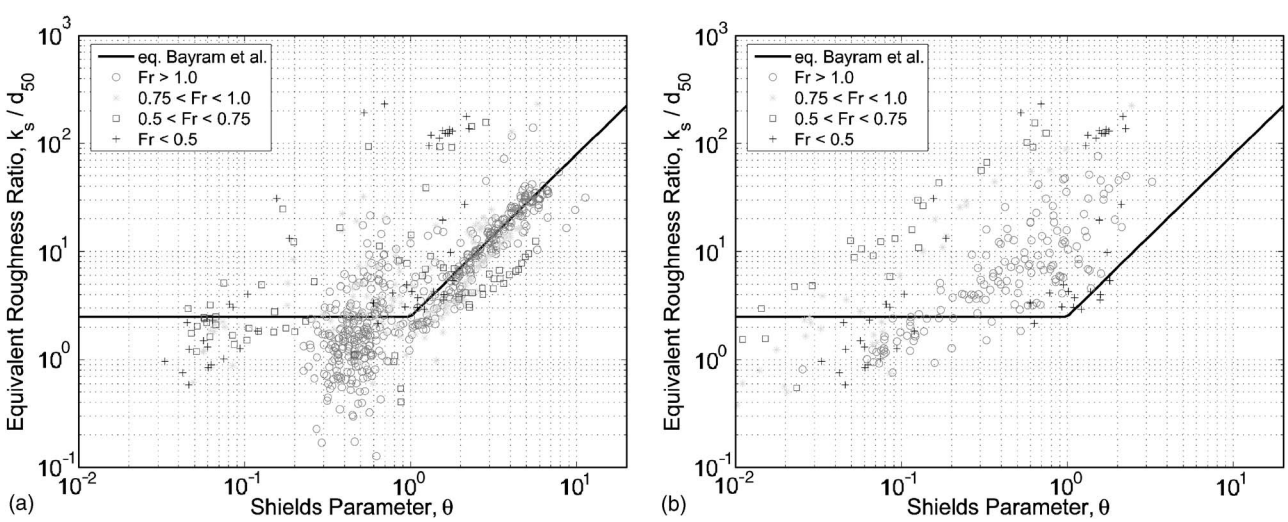

Fig. 8. Equivalent roughness ratio k_s/d_{50} versus total shear stress θ with respect to Froude number together with Bayram et al. formula using data sets where $W_{s*} \leq 10$ (a); or $W_{s*} > 10$ (b)

Table 5. Prediction of Equivalent Roughness within Factor of Two and Five of Measured Values Together with Logarithmic Error Index for Formulas Studied and All Data (Influence of Froude Number)

	$F \leq 1$			$F > 1$		
Author(s)	Pred. ×2 (%)	Pred. ×5 (%)	Er_{log} (%)	Pred. ×2 (%)	Pred. ×5 (%)	Er_{log} (%)
Wilson	28	63	64	58	93	29
Yalin	52	78	46	67	90	28
Van Rijn	55	79	40	61	92	30
Sumer et al.	56	78	43	59	91	32
Bayram et al.	53	80	44	64	91	28
Eq. (15)	68	95	27	77	96	23

in 95% of the experiments). Consequently F should not influence the roughness height for these particular data sets where $W_{s*} < 7$. Table 5 presents errors on equivalent roughness predictions for the different studied formulas with the data separated into subcritical ($F < 1$) and supercritical ($F > 1$) flows. The disagreement displayed by all formulas is substantial for subcritical flow. Formulas studied considerably underestimate the roughness height. Errors in case of $F < 1$ are twice as big as for $F > 1$. Furthermore, considering predictions within a factor of two, only 50% of the data are correctly calculated with these formulas for $F < 1$, whereas approximately 60% of the data are correct for $F > 1$. Similarly, within a range of a factor of five, the percentage of correctly predicted values drops from more than 90% for $F > 1$ to less than 80% for $F < 1$. Simultaneously, the logarithmic error index increases from approximately 30 to 40%.

Larger values of the roughness height than predicted, obtained in the case of subcritical flow, could be explained from the point of view of the small velocities (with respect to the water depth). In the subcritical regime, even for a rough turbulent flow, the velocity profile is easily influenced by nonlinearity induced by the movable bottom. Moreover, Yalin (1977) argued that, based on velocity profiles determined for the central part of flows with a large width/depth ratio, it appears that the logarithmic velocity distribution should be valid up to the free surface of a two-dimensional flow (to the center line for a circular pipe). In Eq. (7), it is assumed that the velocity profile is valid over the entire water depth. The validity of the logarithmic profile over the water depth was observed by Smart (1999, data with subcritical flow). On the other hand, Sumer et al. (1996) observed a relatively thin logarithmic layer (data with supercritical flow). Thus, the Froude number may play a role for the height $h' \leq h$ to which the velocity profile is valid (for free surface flow). As a consequence, k_s may be a function of the Froude number.

New Formula for Roughness Height

The main objective in the present study is to develop a new relationship that can perform satisfactorily under a wide range of conditions. The following equation was based on the previously discussed analysis:

$$\frac{k_s}{d_{50}} = 0.6 + 1.8\left(\frac{W_{s*}^{1.2}}{F^{2.4}}\right)\theta^{1.7} \tag{15}$$

Fig. 9 indicates that the roughness height for the Nnadi and Wilson (1992) and Julien and Raslan (1998) data is still underestimated by Eq. (15). However, it should be kept in mind that in the case of the Nnadi and Wilson data set, since it was obtained in a pressurized closed conduit experiment, the effect of the Froude number has no physical meaning. Eq. (15) is thus not really adequate for this kind of experiments, at least not motivated from a physical point of view, although seen as a relationship based purely on empirical analysis it may be applicable. Nevertheless, Eq. (15) presents results much more accurate than previous relationships for most of the data sets. In Tables 3–5, it is clearly demonstrated that Eq. (15) gives the best results for all measures of accuracy employed. It should also be noted that Eq. (15) gives a good prediction for the lower plane-bed regime (slightly overestimates for the Yalin data) where the roughness height was also found to be proportional to the water depth when the relative depth was small ($h/d_{90} < 10$).

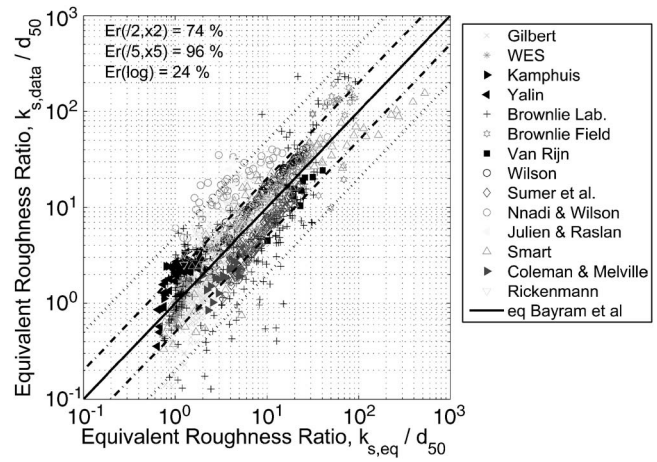

Fig. 9. Comparison between equivalent roughness ratio k_s/d_{50} obtained from data and corresponding values computed with Eq. (15)

Fig. 10 shows that the distribution of the difference $\Delta \log[k_s = \log(k_{s,\text{pred}}) - \log(k_{s,\text{meas}})]$ roughly follows a Gaussian probability function, which implies that errors correspond mainly to experimental uncertainties. As discussed before, a small experimental error may induce large uncertainty in the estimation of k_s.

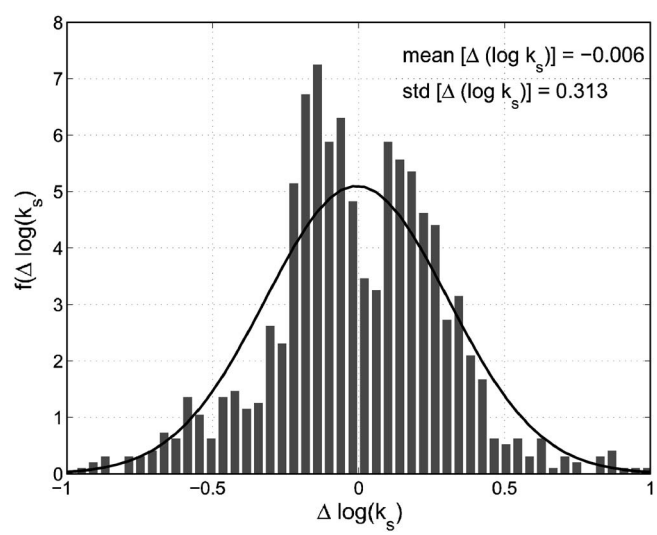

Fig. 10. Distribution of difference $\Delta \log[k_s = \log(k_{s,\text{pred}}) - \log(k_{s,\text{meas}})]$ (black line corresponds to Gaussian function)

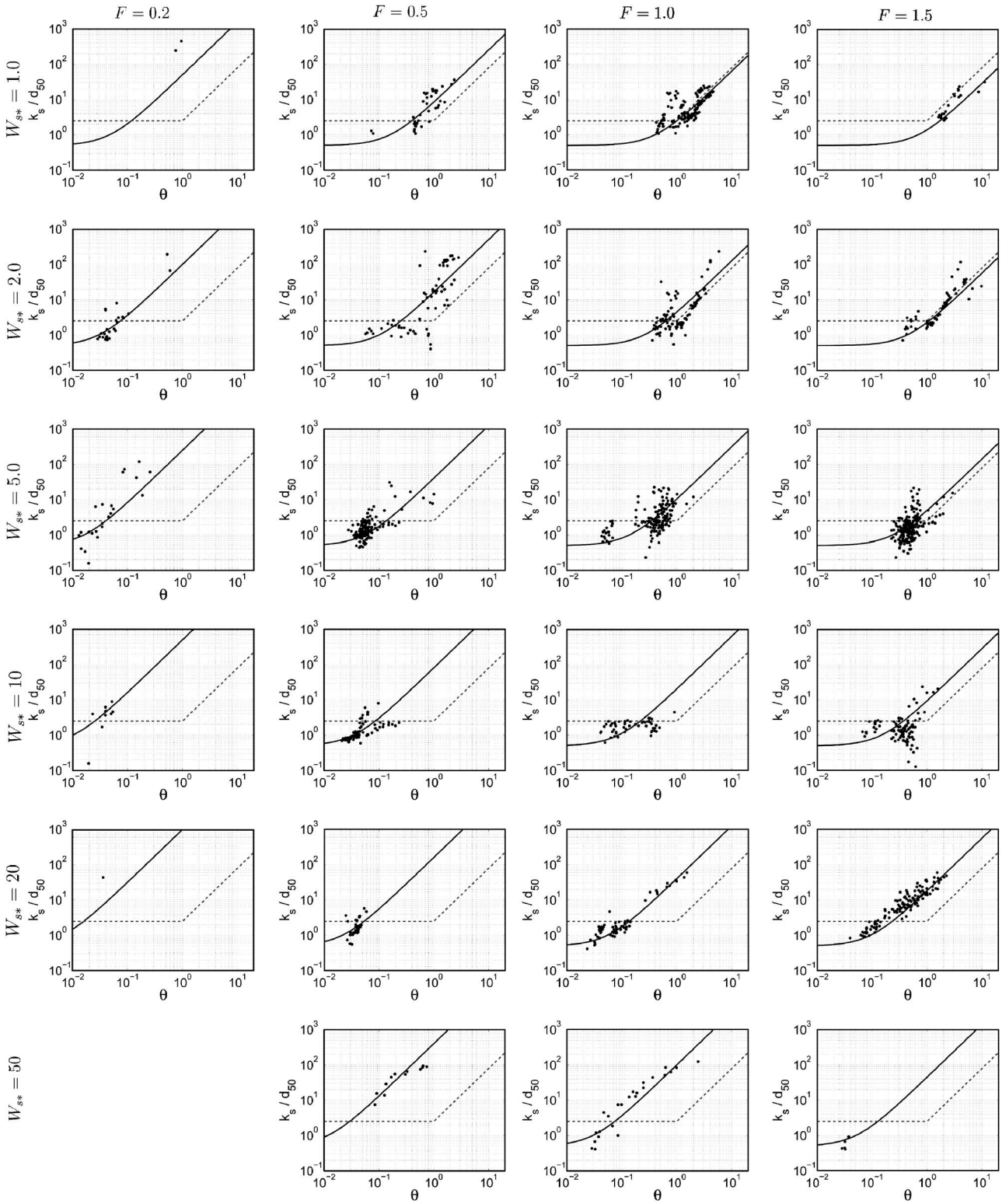

Fig. 11. Dimensionless roughness height versus total Shields parameter for different values of Froude number F and dimensionless settling velocity W_{s*} [full line, dashed line, and points correspond to Eq. (15), Eq. (6), and experimental data, respectively]

Critical Shields Parameter for Upper Plane-Bed Regime

Finally, by introducing a critical Shields parameter for upper plane-bed regime $\theta_{cr,ur}$ such that when $\theta=\theta_{cr,ur}$, $k_s/d_{50}=3$, Eq. (15) can be written

$$\frac{k_s}{d_{50}} = 0.6 + 2.4\left(\frac{\theta}{\theta_{cr,ur}}\right)^{1.7} \tag{16}$$

where the critical Shields parameter for the upper plane regime is defined as

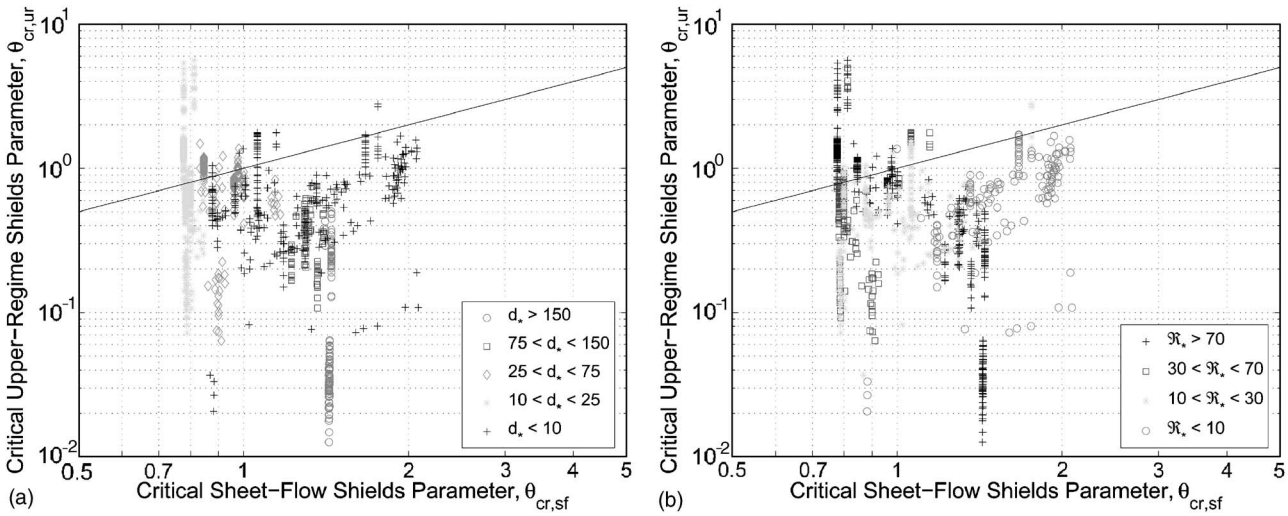

Fig. 12. Prediction of critical Shields parameter for upper regime using new formula [Eq. (17)] versus critical Shields parameter for sheet-flow regime using formula proposed Van Rijn formula [(1984), see Eq. (6)] for different range of values of dimensionless grain size d_* (a); grain shear Reynolds number R_* (b)

$$\theta_{cr,ur} = 1.18\frac{\mathsf{F}^{1.40}}{W_{s*}^{0.70}} \tag{17}$$

Fig. 11 displays in a direct way the significant improvement of the roughness height prediction using Eq. (15) (bold line) compared to existing formulas (the Bayram et al. formula is also presented in Fig. 11; the dashed line). The proportionality of the roughness height to the Shields parameter (to the power 1.7) after the critical Shields parameter for the upper plane-bed regime is reached is clearly illustrated in Fig. 11.

In Fig. 12, it can be observed that the predictions of the upper regime limit using Eq. (17) or the formula proposed by Van Rijn for the inception of the sheet-flow regime [$\theta_{cr,sf}=26\theta_{cr}$, see Eq. (6)] give considerably different results. Except for a few cases with relatively fine sediments ($d_*<30$), Eq. (17) overall predicts smaller values than Eq. (6). A similar behavior (i.e., an increasing function of θ_{cr}) is only observed for the data in the range $\mathsf{R}_*<12$, corresponding to the smooth regime. The Van Rijn formula is only dependent on d_* [as θ_{cr} is a function of dimensionless grain size d_* only, using the equations proposed by Van Rijn (1984), or Soulsby (1997), whereas the proposed formula is a function of the dimensionless settling velocity W_{s*} and the Froude number F. This confirms the observations of Julien and Raslan (1998) that the critical Shields parameter for the upper regime $\theta_{cr,ur}$ is not only a function of θ_{cr} (critical Shields parameter for the inception of movement) but also of F. For low values of the shear Reynolds number [$\mathsf{R}_*<10$, which corresponds to a hydraulically smooth boundary; cf. Fig. 12(b)], it appears that Eq. (17) is also proportional to the critical Shields number for the inception of movement (namely a function of d_* only) as Julien and Raslan (1998) observed previously. However for a hydraulically rough boundary ($\mathsf{R}_*>30$), which is the main assumption of this study, the opposite tendency can be noticed: Eq. (17) is a decreasing function of θ_{cr}. However, the Van Rijn formula [Eq. (6)] is only based on sheet-flow experiments and was developed to predict the inception of sheet flow. Eq. (17) should be employed to predict the inception of the upper plane-bed regime, i.e., where the sediment transport (or/and sheet-flow layer) significantly modify the roughness height.

Different Bed Regimes

Using the critical Shields parameter $\theta_{cr,ur}$ and the suspension parameter ϖ_s, it appears to be possible to separate the three different regimes discussed in "Different Plane-Bed Regimes." In Fig. 13 the suspension parameter is plotted versus the ratio $\theta/\theta_{cr,ur}$. The three different regimes can be differentiated as follows:

- The lower plane-bed regime occurs when $\theta<\theta_{cr,ur}$;
- The upper plane-bed regime without suspension occurs when $\theta>\theta_{cr,ur}$ and $\varpi_s>0.8-1$; and
- The upper plane-bed regime with suspension (suspension sheet flow regime) occurs when $\theta>\theta_{cr,ur}$ and $\varpi_s<0.8-1$.

It can also be observed that $W_{s*}=10$ when the upper regime is reached ($\theta>\theta_{cr,ur}$) is more or less equivalent to $\varpi_s=0.8-1$, which can be employed to separate between the suspension mode upper regime and the no-suspension mode upper regime. Since the parameter W_{s*} does not itself include any quantity characterizing the

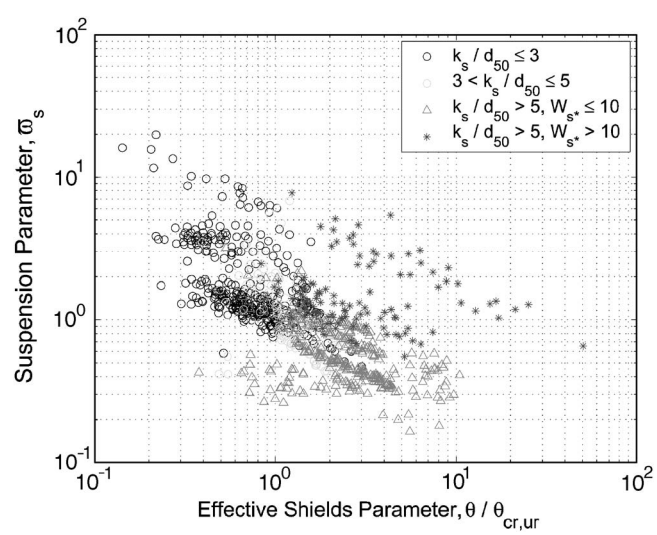

Fig. 13. Suspension parameter versus Shields parameter divided by critical Shields parameter

magnitude of the flow/flow turbulence (which is characterized by the ratio $\theta/\theta_{cr,ur}>1$), it is probable that the suspension sheet-flow regime only occurs for the relatively fine sediment and for fine sediments ($W_{s*}\leq 10$), the no-suspension mode in the upper regime seems to seldom occur as the suspension mode is often reached as soon as the upper regime is reached. On the other hand, for coarser sediments ($W_{s*}>10$), the suspension mode appears not to occur as easily.

Finally, it should be noted that the condition for the lower plane-bed regime ($\theta<\theta_{cr,ur}$) is necessary but not sufficient. Indeed, the critical Shields parameter for the upper regime should correspond to the disappearance of the bed forms. Thus, for $\theta<\theta_{cr,ur}$, bed forms may appear. In that case, the method of Soulsby (1997) may be used, i.e., the geometry of the bed forms and the induced roughness height should be calculated using existing empirical relationships, and the total roughness may be obtained by adding the two values: $k_{s,\text{total}}=k_s+k_{s,\text{bed forms}}$ [where k_s is obtained using Eq. (16), $0.6<k_s<3$ if $\theta<\theta_{cr,ur}$].

Conclusions

In the present study, data from many sources were compiled and analyzed to determine the roughness height for the plane-bed regime. Based on this analysis, the following conclusions were drawn:

1. Flow resistance for plane beds under steady currents can be expressed in terms of the ratio of Nikuradse's equivalent sand roughness to the grain diameter, k_s/d_{50}, given as a function of the Shields parameter based on the total shear stress, the Froude number, and the dimensionless settling velocity.
2. Flow resistance data can be represented by the new equation [Eq. (15)] for both lower and upper plane-bed regimes (with or without suspension).
3. The separation between the lower and upper plane-bed regimes is reasonably well described by the critical Shields parameter $\theta_{cr,ur}$ which is a function of the Froude number F and the dimensionless settling velocity W_{s*}. For the lower plane-bed regime, the roughness height may only be a function of the grain size. However, as soon as the upper plane-bed regime is reached, the roughness height is proportional to the Shields parameter to the power 1.7.
4. A relationship between the roughness height and the total Shields parameter makes iterative computations necessary in practical applications. Such a method could imply large discrepancies in the results compared to the direct fitting using measured data, and thus might need some modifications.

Acknowledgments

This work was conducted in part under the Inlet Modeling System Work Unit of the Coastal Inlets Research Program, U.S. Army Corps of Engineers and in part under the HUMOR program supported by the European Community.

Notation

The following symbols are used in this paper:

A_b = constant;
b = flume or river width;
d = sand diameter (grain size);
d_{50}, d_{90} = median sand diameter and diameter for which 90% of sediment by weight is smaller, respectively;
d_* = dimensionless grain size;
F = Froude number;
g = acceleration due to gravity;
h = water depth;
I_e = energy slope;
k_s = roughness height;
Q = flow discharge;
R_b = hydraulic radius associated with bed;
R_* = grain shear Reynolds number ($\mathsf{R}_*=u_*d_{50}/\nu$);
R_{*b} = grain shear Reynolds number ($\mathsf{R}_{*b}=u_*k_s/\nu$);
T = transport stage parameter proposed by Van Rijn;
U_c = mean velocity ($U_c=Q/bh$);
u = horizontal velocity;
u_* = friction velocity;
W_s = settling velocity;
W_{s*} = nondimensional settling velocity [$W_*=(s-1)^{2/3}/(g\nu)^{1/3}W_s$];
W_* = nondimensional settling velocity proposed by Sumer et al. [$W_*=W_s/\sqrt{(s-1)gd_{50}}$];
z_0 = roughness length ($z_0=k_s/30$);
θ = total Shields parameter due to steady current;
θ_{cr} = critical Shields parameter for inception of motion;
$\theta_{cr,ur}$ = critical Shields parameter for inception of upper plane-bed regime;
κ = von Karman constant;
ν = kinematic water viscosity ($\nu=10^{-6}$ m^2/s); and
ϖ_s = suspension parameter ($\varpi_s=W_s/u_*$).

References

Ahrens, J. (2000). "The fall-velocity equation." *J. Waterway, Port, Coastal, Ocean Eng.*, 126(2), 99–102.

Bayram, A., Camenen, B., and Larson, M. (2003). "Equivalent roughness under sheet flow conditions." *Proc. Coastal Sediments 03* (CD-ROM), ASCE, Clearwater Beach, Fla.

Brownlie, W. (1981). "Compilation of alluvial channel data: Laboratory and field." *Technical Rep. No. KH-R-43B*, California Institute of Technology, Pasadena, Calif.

Colby, B., and Hembree, C. (1955). "Computations of total sediment discharge, Niobrara river near Cody, Nebraska." *Technical Rep. No. 1357*, U.S. Geological Survey, Washington, D.C.

Coleman, S., and Melville, B. (1996). "Initiation of bed forms on a flat sand bed." *J. Hydraul. Eng.*, 122(6), 301–310.

Culbertson, J., Scott, C., and Bennet, J. (1972). "Alluvial-channel data from Rio Grande conveyance channel. New Mexico, 1965–69.." *Technical Rep. No. 562-J*, U.S. Geological Survey, Washington, D.C.

Einstein, H., and Chien, N. (1955). "Effects of heavy sediment concentration near the bed on velocity and sediment distribution." *Technical Rep. No. 8*, Inst. of Engineering Res., Univ. of California, Calif.

Ferro, V., and Baiamonte, G. (1994). "Flow velocity profile in gravel-bed rivers." *J. Hydraul. Eng.*, 120(1), 60–80.

Gilbert, G. (1914). "The transportation of debris by running water." *Technical Rep. No. 86*, U.S. Geological Survey, Washington, D.C.

Guy, H., Simmons, D., and Richardson, E. (1966). "Summary of alluvial channel data from flume experiment 1956–1961." *Technical Rep. No. 462-I*, U.S. Geological Survey, Washington, D.C.

Julien, P., and Raslan, Y. (1998). "Upper-regime plane bed." *J. Hydraul. Eng.*, 124(11), 1086–1096.

Kamphuis, J. (1974). "Determination of sand roughness for fixed beds."

J. Hydraul. Res., 12(2), 193–203.
Neill, C. (1967). "Laboratory study of scour of coarse uniform bed material." *Technical Rep.*, Research Council of Alberta, Alberta, Canada.
Nikora, V., and Smart, G. (1997). "Turbulence characteristics of New Zealand gravel-bed rivers." *J. Hydraul. Eng.*, 123(9), 764–773.
Nnadi, F., and Wilson, K. (1992). "Motion of contact-load particles at high shear stress." *J. Infastruct. Finance*, 118(12), 1670–1684.
Rickenmann, D. (1991). "Hyperconcentrated flow and sediment transport at steep slopes." *J. Hydraul. Eng.*, 117(11), 1419–1439.
Schlichting, H. (1979). *Boundary layer theory*, McGraw–Hill, New York.
Singh, B. (1960). "Transport of bed-load in channels with special reference to gradient form." Ph.D. thesis, Univ. of London, London.
Sleath, J. (1984). *Sea bed mechanics*, Wiley-Interscience, New York.
Smart, G. (1984). "Sediment transport formula for steep channels." *J. Hydraul. Eng.*, 110(3), 267–276.
Smart, G. (1999). "Turbulent velocity profiles and boundary shear in gravel bed rivers." *J. Hydraul. Eng.*, 125(2), 106–116.
Smart, G., Duncan, M., and Walsh, J. (2002). "Relatively rough flow resistance equations." *J. Hydraul. Eng.*, 128(6), 568–578.
Song, T., Graf, W., and Lemmin, U. (1994). "Uniform flow in open channels with movable gravel bed." *J. Hydraul. Res.*, 32(6), 861–876.
Soulsby, R. (1997). *Dynamics of marine sands. A manual for practical applications*, Thomas Telford, London.
Sumer, B., Kozakiewicz, A., Fredse, J., and Deigaard, R. (1996). "Velocity and concentration profiles in sheet-flow layer of movable bed." *J. Hydraul. Eng.*, 122(10), 549–558.
U.S. Waterways Experiment Station. (1935). "Studies of river bed materials and their movement with special reference to the lower Mississippi River." *Technical Rep. No. 17*, U.S. Army Corps of Engineers, Vicksburg, Miss.
U.S. Waterways Experiment Station. (1936). "Flume tests of synthetic sand mixture (Sand No. 10)." *Technical Memorandum 95-1*, U.S. Army Corps of Engineers, Vicksburg, Miss.
Van Rijn, L. (1984). "Sediment transport. I: Bed load transport." *J. Hydraul. Eng.*, 110(10), 1431–1456.
Van Rijn, L. (1993). *Principles of sediment transport in rivers, estuaries, and coastal seas*, Aqua, The Netherlands.
Whiting, P., and Dietrich, W. (1990). "Boundary shear stress and roughness over mobile alluvial beds." *J. Hydraul. Eng.*, 116(12), 1495–1511.
Williams, G. (1970). "Flume width and water depth effects in sediment transport experiments." *Technical Rep. No. 562-H*, U.S. Geological Survey, Washington, D.C.
Willis, G., Coleman, N., and Ellis, W. (1972). "Laboratory study of transport of fine sand." *J. Hydr. Div.*, 98(3), 801–816.
Wilson, K. (1966). "Bed-load transport at high shear stress." *J. Hydr. Div.*, 92(11), 49–59.
Wilson, K. (1987). "Analysis of bed-load motion at high shear stress." *J. Hydraul. Eng.*, 113(1), 97–103.
Wilson, K. (1989). "Mobile-bed friction at high shear stress." *J. Hydraul. Eng.*, 115(6), 825–830.
Winterwerp, J., De Groot, M., Mastbergen, D., and Verwoert, H. (1990). "Hyperconcentrated sand-water mixture flows over flat bed." *J. Hydraul. Eng.*, 116(1), 36–54.
Wu, W., and Wang, S. (1999). "Movable bed roughness in alluvial rivers." *J. Hydraul. Eng.*, 125(12), 1309–1312.
Yalin, M. (1977). *Mechanics of sediment transport*, 2nd Ed., Pergamon, Oxford, U.K.
Yalin, M. (1992). *River mechanics*, Pergamon, Oxford, U.K.